RESEARCH ARTICLE

Impact of Urbanization on Urban Heat Island and Urban Thermal Field Variance Index of Coastal City Surabaya, Indonesia between 2005 and 2020

Risma Salsabila Foresty[1], **Rida Ayu Surya Putri**[1], **Ririn Nur Fadhilah**[1], **Salma Kamiliya Fatin**[1], **Muhammad Nur Sulton**[1], and **Ahmad Dwi Setyawan**[1,2,*]

[1]Department of Environmental Science , Faculty of Mathematics and Natural Sciences, Sebelas Maret University Jl. Ir. Sutami 36A Surakarta 57126, Central Java, Indonesia
[2]Biodiversity Research Group, Sebelas Maret University. Jl. Ir. Sutami 36A, Surakarta 57126, Central Java, Indonesia

*Corresponding author: Ahmad Dwi Setyawan, volatileoils@gmail.com

Article Information

Article History:
Received: 3 June 2024
Revised: 18 September 2024
Accepted: 14 October 2024
Published: 22 October 2025

Keywords:
Land Surface Temperature
Surabaya
Urban Heat Island
Urban Thermal Field Variance Index
Urbanization

Abstract

The city of Surabaya serves as the capital of East Java Province, Indonesia, experiencing the most intensive anthropogenic activities in this province. It has emerged as a primary destination for urbanization from various regions, leading to notable shifts in land use, vegetation, and Land Surface Temperature (LST). This study aims to analyzing the impact of urbanization on urban heat island and urban thermal field variance of coastal city Surabaya, Indonesia between 2005 and 2020. The findings reveal that Land Use Land Cover (LULC) changes significantly impact LST in Surabaya. Pearson Correlation results showed a positive correlation between Normalized Difference Vegetation Index, Urban Thermal Field Variance Index, and Urban Heat Island in 2005, 2011, 2015 and 2020 ($p < 0.01$). Alterations in land use contribute to elevated surface temperatures owing to diminished vegetation and increased built-up areas, thereby exacerbating ecological degradation and posing health risks to the urban environment. Consequently, implementing mitigation and adaptation measures becomes imperative to address the escalating urban heat phenomenon. Strategies such as augmenting green infrastructure and optimizing blue infrastructure are crucial for maintaining thermal equilibrium across the urban landscape.

1. Introduction

Urbanization denotes the transition from rural to urban areas characterized by heightened population density and improved infrastructure (Wu et al., 2023). It is propelled by escalating population growth and rapid development, influenced by social, economic, demographic, and environmental factors (Moazzam et al., 2022; Ji et al., 2023). The ramifications of urbanization are diverse, encompassing alterations in vegetation (Ji et al., 2023), land cover and use (Moazzam et al., 2022), modulation of land surface temperatures (Seun et al., 2022), and heightened greenhouse emissions. Changes in land cover and increased land use stem from construction activities, road infrastructure expansion, and growing demand for amenities (Chairuman et al., 2023), impacting urban temperatures (Choudhury et al., 2019) and Land Surface Temperature (LST). Diminished land cover in urban locales leads to higher temperatures compared to rural areas (Safitri et al., 2022), attributed to heightened human activity resulting in increased heat release (Khanh et al., 2023). LST exhibits a significant correlation with Urban Heat Island (UHI), where UHI denotes a phenomenon in which urban areas retain and absorb more heat than their surroundings (Rahardian and Ruslana, 2022), primarily due to intensified human activity such as construction and emissions (Ziar et al., 2019). Building construction, characterized by low albedo surfaces, absorbs solar radiation and heat energy, contributing to heat buildup (Noviyanti and Santoso, 2016), while reducing vegetation diminishes the cooling effect facilitated by the evapotranspiration process (Sasmito and Suprayogi, 2017), indirectly elevating LST.

ISSN 3088-1803

Surabaya, with its rich cultural, historical, and trade heritage, witnesses rapid changes in land cover types driven by surging population growth rates (Faza Illiyin et al., 2019). The city's reputation as a hot urban center stems from its pronounced urbanization, leading to a surge in its population (Katherina and Indraprahasta, 2019). Surabaya's status as the capital of East Java Province, Indonesia, bolstered by governmental, economic, tourism, cultural, and educational prowess, underscores its allure for urbanization (Katherina and Indraprahasta, 2019). Continued development to meet burgeoning human needs transforms green spaces into commercial, industrial, and transportation infrastructures, impeding water absorption and exacerbating heat retention (Syafitri et al., 2021). The proliferation of large-scale, high-density constructions further worsens temperature trapping and urban heat (Syafitri et al., 2021). Persistent urbanization and development portend a significant rise in regional temperatures, epitomized by UHI, amplifying energy consumption and air conditioning demands in Surabaya (Sari, 2021). As in the study conducted by Yin et al. (2023) which showed that the increase in population increased the urban heat island and discomfort in the New York City area by 50%. Understanding the nexus between land use and land cover changes attributable to urbanization and rising surface temperatures serves as a blueprint for formulating land use mechanisms, development planning, policy formulation, and land use evaluation (Pan et al., 2023).

The objectives of this study were as follows:

1. To ascertain the impact of Land Use Land Cover (LULC) changes on LST utilizing Landsat-7 and Landsat-8 remote sensing analysis.
2. To establish correlations between LST and Normalized Difference Vegetation Index (NDVI), Normalized Difference Built-Up Index (NDBI), UHI, and Urban Thermal Field Variance Index (UTFVI).
3. To devise mitigation and adaptation strategies in response to UHI trends.

2. Materials and Methods

2.1 Study Area

The study was conducted in the Surabaya City area, which is the capital of East Java Province, Indonesia (Fig. 3). This city exhibits a high degree of urbanization and rapid development (Kurniati and Nitivattananon, 2016). Geographically, this region lies between 7°9′–7°21′ South latitude and 112°36′–112°57′ East longitude (Kurniati and Nitivattananon, 2016), and covers an area of approximately 335.28 km^2, comprising 31 districts and 154 sub-districts with a population of more than 3 million (Khafid et al., 2020). Surabaya City experiences an average temperature ranging from 26.07°C to 29.03°C, with humidity levels between 35% and 99%. Additionally, the city receives significant rainfall throughout the year, totaling 551.8 mm. Land use in Surabaya is varied, including residential areas, commercial and service sectors, as well as green open spaces (Kusuma et al., 2020).

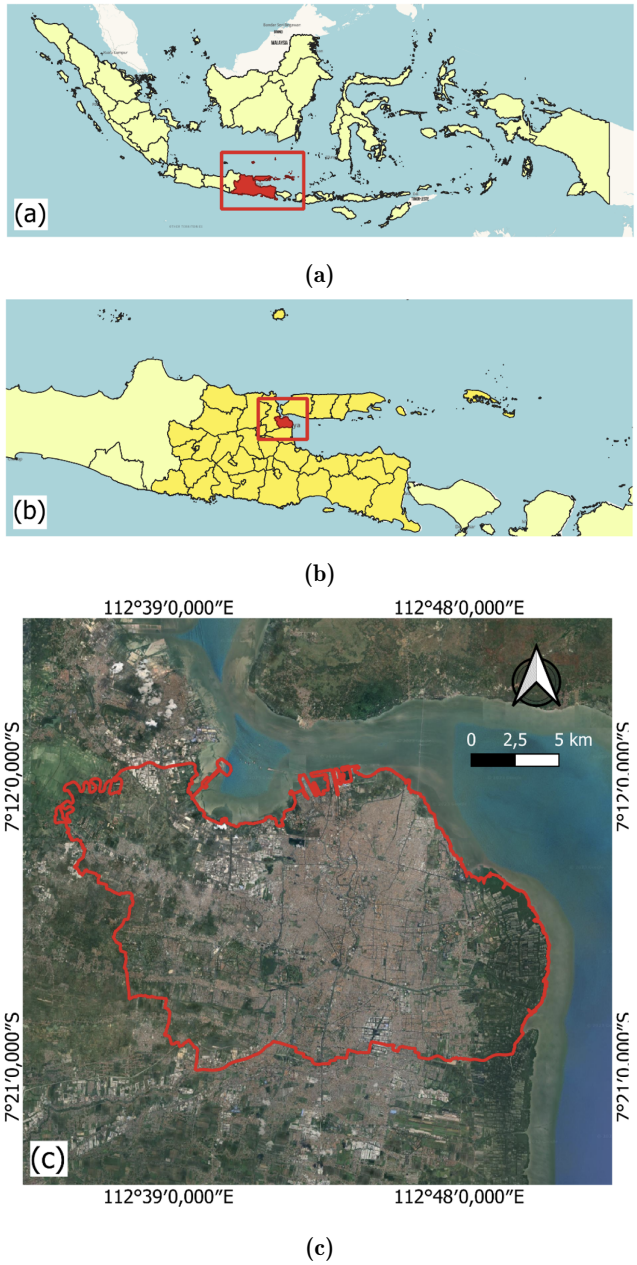

Figure 1. Maps of the study area: (a) East Java Province, Indonesia; (b) Surabaya City; (c) Satellite image of Surabaya City.

2.2 Data Source and Pre-processing

This study utilized Landsat-7 satellite image data for the years 2005 and 2011, along with Landsat-8 data for 2015 and 2020 (Table 1). The dataset spans five years across four time periods. However, data from

2010 was excluded due to unsatisfactory image quality, primarily attributed to significant cloud cover. Consequently, the 2011 image was utilized as a substitute. The data were procured from the US Geological Survey (USGS) via earthexplorer.usgs.gov, ensuring cloud cover was less than 10%. These satellite images facilitated analysis of LULC, LST, UHI, UTFVI, NDVI, and NDBI within the Surabaya city limits. Image preprocessing encompassed radiometric and atmospheric correction, as well as brightness temperature extraction from Landsat images using QGIS version 3.28.11 software, complemented by the Semi-automatic Classification Plugin (SCP) developed by Congedo (2021). The SCP facilitated various remote sensing data processing tasks, including data downloading, image preprocessing, image classification and analysis, and postprocessing to enhance data interpretation and classification accuracy (Tempa and Aryal, 2022). Specifically, in this study, SCP was instrumental in the pre-processing phase of Landsat images, notably for atmospheric corrections aimed at mitigating cloud interference and minimizing the impact of thin fog present in the images.

Table 1. Landsat images used in this research.

Satellites / Sensors	Acquisition Date (YY/M-M/DD)	Path / Row	Spatial Resolution of Spectral Bands (m)	Spatial Resolution of TIR Band (m)	Cloud Cover (%)
Landsat-7 ETM+	2005-03-08	118/65	30	60	9.00
Landsat-7 ETM+	2011-09-01	118/65	30	60	2.00
Landsat-8 OLI	2015-06-16	118/65	30	100	0.24
Landsat-8 OLI	2020-07-31	118/65	30	100	4.98

2.3 Experimental Design

The acquired dataset underwent processing in ArcGIS® version 10.8 to assess the presence of UHI phenomenon within Surabaya. This analysis aimed to determine the values of the NDVI, NDBI, and LST. The land cover classification involved categorizing LULC using sample points for each land cover type —urban, green space, and water— utilizing the Maximum Likelihood Classification tool (Saputra et al., 2023). Subsequently, LULC accuracy was assessed using Google Earth Pro with sample points created by a confusion matrix to ascertain accuracy percentages.

Calculation of NDVI, NDBI, and LST values was conducted using a raster calculator with thermal bands, according to their respective functions within the Landsat image dataset (Fig. 2). This is done to find out the relationship between UTFVI and UHI, but other comparisons are needed in the form of NDVI, NDBI, LST, LULC. Determination of UHI values entailed LST calculations, incorporating raster values alongside minimum temperature values (Bala et al., 2021). Furthermore, the calculation of UTFVI involved computing LST and mean LST values to derive the Ecological Evaluation Index (EEI) for Surabaya city. Subsequently, variables such as NDVI, NDBI, UHI, LST, and UTFVI underwent Pearson correlation analysis using IBM Statistics SPSS® version 22 software to elucidate statistical conclusions and interrelationships among the variables (Alademomi et al., 2022).

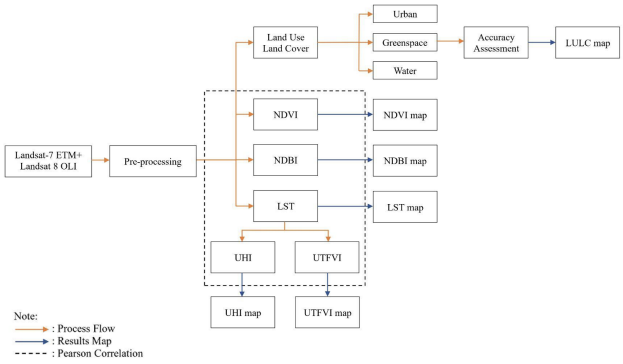

Figure 2. Flowchart of the methodology.

2.4 Computation of Land Use Land Cover

Remote sensing, utilizing Landsat imagery, is instrumental in mapping land cover and its temporal changes across various class classifications (Karakuş, 2019). The city of Surabaya was classified into three distinct categories based on land use —urban, green space, and water— during the years 2005, 2011, 2015, and 2020 (Table 2). Urban Classification uses a "false color" composition where densely populated urban areas are shown in light blue. This combination of TM bands gives results similar to traditional color infrared aerial photography. The water band combination is used to distinguish land from water. In the image, ice will appear as bright magenta, land will appear as green and orange, and water will appear as shades of blue. With this band combination, vegetation type and condition show as variations of hues (browns, greens and oranges), as well as in tone. This combination of bands is called infrared color because chlorophyll reflects near infrared light, the composition of this band is useful for analyzing vegetation. Specifically, the red areas have better vegetation. Dark areas are water and urban areas are white. Notably, the year 2010 was excluded from LULC classification due to high cloud cover rendering image results unusable, hence the 2011 image was utilized as a replacement. This classification process was executed using ArcGIS 10.8 and Google Earth Pro software, employing sample points to ascertain accuracy (Islami et al., 2022). The kappa accuracy test was employed to compare classified satellite image data with field data obtained from Google Earth Pro (Dash et al., 2023). Accuracy points were generated randomly in ArcGIS 10.8 using a confusion matrix to establish truth levels, yielding Kappa points (Alademomi et al., 2022). Accuracy was calculated by dividing the number of pixels classified in each class by the total number of pixels tested for that class, thereby representing the percentage of correct classifications (Olofsson et al., 2014). LULC in the city of Surabaya was

delineated into three primary land cover classes: urban, green space, and water (Taufik et al., 2016).

Table 2. Description of LULC classes in the Surabaya City research area.

LULC	Information
Urban	All built-up areas, including residential, commercial, industrial, transportation infrastructure, and villages.
Green Space	Agricultural areas, plantations, grasslands, cemeteries, natural forests, bare areas, fields, and mangrove forests.
Water	All open water areas, including lakes, reservoirs, rivers, ponds, and seas.

2.5 Retrieval of Land Surface Temperature

Land Surface Temperature (LST) was calculated utilizing Landsat data's infrared band to visualize the spatial distribution of surface temperature. Temperature data were extracted from digital images by converting the digital number within satellite imagery, accounting for atmospheric absorption and heat emissions. The resultant surface temperature values in LST calculations were expressed in degrees Celsius (°C). These LST values were then grouped into four distinct classes: the first class encompassed temperatures below 20°C, the second class ranged from 20°C to 25°C, the third class spanned temperatures between 25°C to 30°C, and the final class included temperatures exceeding 30°C (Ullah et al., 2022). The LST is computed using Eq. 1:

$$LST = \frac{T_B}{1 + \left(\frac{\lambda \sigma T_B}{hc}\right) \ln \varepsilon} \tag{1}$$

where

T_B: Brightness temperature

λ: Wavelength

σ: Boltzmann constant (1.38×10^{-23} J/K)

h: Planck constant (6.626×10^{-34} Js)

c: Speed of light in vacuum (2.998×10^{8} m/s)

ε: Emissivity ($0.004 \times P_v + 0.986$)

Spatial autocorrelation analysis is used to describe significant local clustering patterns (Gunathilaka and Harshana, 2021). We use spatial autocorrelation Moran's (I) which has spatial patterns and determines whether the pattern is scattered, clustered, or random based on location and values. This analysis identifies patterns by looking at the z-score and p-value of the index. A p-value greater than 0.05 implies that the data are spatially randomly distributed. Then if the p-value is less than 0.05 with a negative $z < -2.58$ then the data set is spatially distributed. Furthermore, a p-value of less than 0.05 and a positive $z > 2.58$ indicates a clustering pattern of data that is distributed in clusters (Kumari et al., 2019).

2.6 NDVI and NDBI Calculations

The Normalized Difference Vegetation Index (NDVI) serves to assess vegetation cover and detect changes in vegetation (Gandhi et al., 2015). This index is derived from near-infrared calculations based on light reflected by plants (Achmad et al., 2019). NDVI values range from -1 to $+1$, where a value close to 0 indicates poor vegetation cover, such as built-up areas, while a value near $+1$ signifies dense vegetation, such as dense forests, and a value close to -1 represents water bodies (Khamchiangta and Dhakal, 2020). NDVI is computed using Eq. 2:

$$NDVI = \frac{NIR - RED}{NIR + RED} \tag{2}$$

Here, NIR corresponds to Band 4 (Landsat 7) and Band 5 (Landsat 8), while RED corresponds to Band 3 (Landsat 7) and Band 4 (Landsat 8). NDVI classification encompasses four classes (Nailufar, 2018): viz. Class < 0.25 denotes sparse vegetation density, class 0.26–0.45 signifies medium vegetation density, class 0.46–0.59 indicates dense vegetation density, class > 0.60 represents very dense vegetation density (Ullah et al., 2022).

The Normalized Difference Built-up Index (NDBI) is utilized to determine the built-up areas. NDBI values range from -1 to $+1$, with negative values indicating water bodies and positive values indicating developed areas. NDBI is calculated using Eq. 3:

$$NDBI = \frac{SWIR - NIR}{SWIR + NIR} \tag{3}$$

It comprises four classes (Handayani et al., 2017), namely class < -0.99 signifies rare building density, class -0.10 to -0.75 represents medium building density, class -0.76 to -0.45 indicates dense building density, class > -0.46 denotes very dense building density. Here, $SWIR$ utilizes Band 5 (Landsat 7) and Band 6 (Landsat 8), while NIR utilizes Band 4 (Landsat 7) and Band 5 (Landsat 8).

2.7 Mapping Urban Heat Island

Urban Heat Island (UHI) was obtained through a range of LST calculation values (Ullah et al., 2022) using the Eq. 4.

$$UHI = \frac{T - T_{\min}}{T_{\min}} \tag{4}$$

where

T: LST raster value

$T_{\min}$: Minimum temperature value

Table 3 shows the classification of UHI in Surabaya City.

Table 3. Description of UHI classes in the Surabaya City study area (Xiong et al. 2021).

UHI Classification	Class	Value 2005	Value 2011	Value 2015	Value 2020
Very High	Temperature $> u + std$	> 0.81	> 1.01	> 0.71	> 0.42
High	$u + 0.5std <$ Temperature $\leq u + std$	0.745–0.81	0.925–1.01	0.65–0.71	0.37–0.42
Moderate	$u - 0.5std \leq$ Temperature $\leq u + 0.5std$	0.615–0.745	0.755–0.925	0.53–0.65	0.27–0.37
Low	$u - std \leq$ Temperature $< u - 0.5std$	0.8–0.615	0.67–0.755	0.47–0.53	0.22–0.27
UHI No	Temperature $< u - std$	< 0.8	< 0.67	< 0.47	< 0.22

Note: u denotes the mean surface temperature; *std* denotes the standard deviation.

2.8 The Urban Thermal Field Variance Index

The Urban Thermal Field Variance Index (UTFVI) serves as a tool for assessing the impact of Urban Heat Islands (UHI) on urban areas, particularly in evaluating their influence on the quality of life. UTFVI values are derived from existing temperature data and are categorized into five classes:

- Good: $UTFVI < 0.005$
- Normal: $0.005 \leq UTFVI < 0.010$
- Bad: $0.010 \leq UTFVI < 0.015$
- Worse: $0.015 \leq UTFVI < 0.020$
- Worst: $UTFVI \geq 0.020$

By categorizing UTFVI into these classes, it becomes possible to gauge the severity of UHI impact within urban environments, aiding in urban planning and mitigation strategies (Ullah et al., 2022). UTFVI is calculated using Eq. 5:

$$UTFVI = \frac{T_s - T_{\text{mean}}}{T_{\text{mean}}} \tag{5}$$

where

T_s: LST (°C)

T_{mean}: Mean LST (°C)

2.9 Data Analysis

Pearson correlation analysis was conducted using IBM SPSS Statistics version 22 software, with the aim of exploring the relationships between the variables in this study, which include NDBI, UTFVI, UHI, LST, and NDVI (Safitri, 2016). This statistical method involves one dependent variable and one independent variable to generate a correlation coefficient, which measures the strength and direction of the relationship between two variables. The correlation coefficient ranges from -1 to 1, where a value of -1 indicates a perfect negative relationship, suggesting an inversely proportional connection between variables, while a value close to 1 indicates a perfect positive relationship, signifying a directly proportional connection between variables (Chung et al., 2020).

In this study, 262 sample points were randomly collected from images of the aforementioned variables, and the Pearson correlation analysis was employed to identify and quantify relationships within the dataset. The determination of 262 samples was performed using the fishnet tool, which creates a grid or square net in a specific area on a map. This tool was used to support data analysis, such as calculating averages, sums, and other statistics.

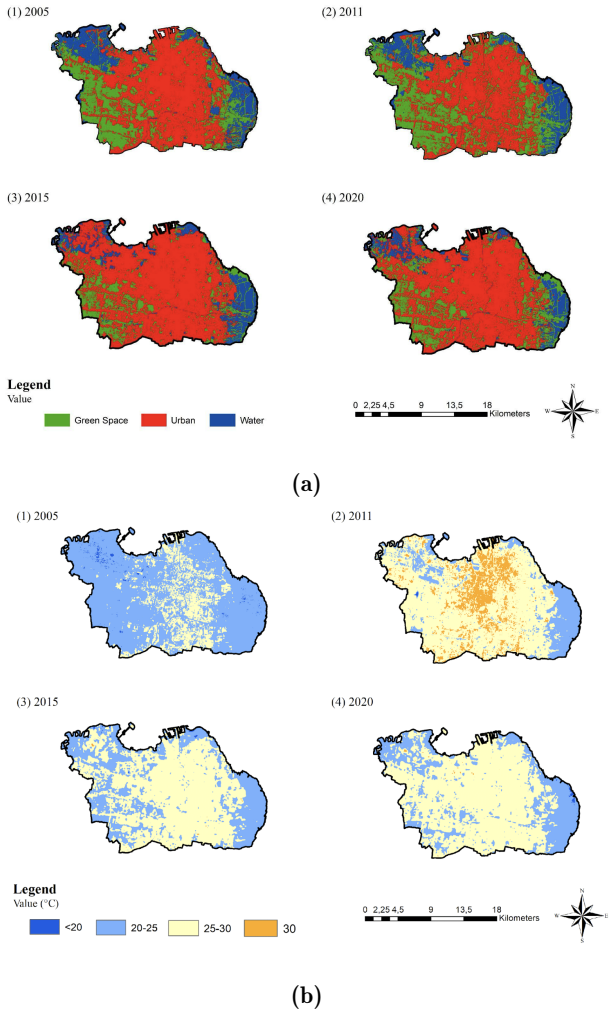

Figure 3. Illustration of (a) land use/land cover (LULC) map of Surabaya City and (b) land surface temperature (LST) map of Surabaya City in 2005, 2011, 2015, and 2020.

Table 4. Details of normalized difference of LULC, NDVI, NDBI, LST, UHI, and UTFVI from 2005 to 2020.

	Classes	Area (Hectares)			
		2005	**2011**	**2015**	**2020**
LULC	Urban	18336.11 (55%)	16348.39 (49%)	23771.48 (71%)	22354.28 (66%)
	Green Space	9813.25 (30%)	12639.38 (38%)	5178.09 (17%)	7830.70 (23%)
	Water	4907.67 (15%)	4070.93 (12%)	4173.92 (12%)	3461.02 (10%)
NDVI	< 0.25	20837.46	24134.53	14082.62	15967.37
	0.26–0.45	7183.75	8279.59	11375.89	10038.27
	0.46–0.59	4054.47	1104.62	4870.43	4621.21
	> 0.60	1588.80	145.69	3333.60	3035.70
NDBI	< -0.99	817.21	288.36	1728.31	1571.48
	-0.10 – -0.75	13428.25	5995.69	13088.11	11309.23
	-0.76 – -0.45	17228.00	25180.96	15971.53	20619.63
	> -0.46	2189.39	2199.24	2875.81	162.48
LST	$< 20°C$	247.7 (0.74%)	16.2 (0.05%)	59.53 (0.18%)	75.46 (0.22%)
	20–25°C	26720.25 (79.36%)	5794 (17.21%)	12181.68 (36.18%)	9864.7 (29.30%)
	25–30°C	6701.27 (19.90%)	22864.49 (67.91%)	21408.94 (63.59%)	23688.13 (70.36%)
	$> 30°C$	1.11 (0.00%)	4993.43 (14.83%)	18.92 (0.06%)	38.95 (0.12%)
UHI	No UHI	5223.95 (15.52%)	2373.53 (7.05%)	3861.16 (11.47%)	3037.67 (9.02%)
	Low	8759.88 (26.02%)	3440.20 (10.22%)	4960.21 (14.73%)	4329.97 (12.86%)
	Moderate	6833.39 (20.3%)	5469.73 (16.25%)	7390.01 (21.95%)	7778.18 (23.11%)
	High	9507.40 (28.24%)	10859.55 (32.26%)	9300.40 (27.63%)	11188.13 (33.24%)
	Very High	3337.26 (9.91%)	11521.07 (34.22%)	8152.14 (24.22%)	7329.42 (21.77%)
UTFVI	< 0.005	5223.95 (20.98%)	13.88 (0.04%)	4255.81 (12.64%)	3028.23 (9%)
	0.005–0.010	8759.88 (35.18%)	3512.06 (10.43%)	5530.82 (16.43%)	4295.81 (12.76%)
	0.010–0.015	6833.39 (27.44%)	6046.66 (17.96%)	7789.92 (23.14%)	7906.67 (23.49%)
	0.015–0.020	9507.40 (38.18%)	12576.10 (37.36%)	9268.19 (27.53%)	11332.01 (33.66%)
	> 0.020	3337.26 (13.40%)	11514.45 (34.20%)	6819.90 (20.26%)	7100.99 (21.09%)

3. Experimental Results

3.1 Land Use Cover and Changes Analysis

The spatially detailed map (Fig. 3a) delineates three LULC categories, namely urban, green space, and water, for the years 2005, 2011, 2015, and 2020. Table 4 provides the sizes of the urban area, green space, and water bodies in hectares (Ha). Additionally, Table 4 presents the distribution of urban areas, green spaces, and water bodies in percentage form.

Table 4 illustrates that changes in the urban area from 2005 to 2020 were relatively insignificant. Notably, from 2005 to 2011, there was a decrease in the urban area from 18,336.11 ha to 16,348.39 ha. Conversely, between 2011 and 2015, the urban area expanded from 16,348.39 ha to 23,771.48 ha, followed by a subsequent reduction from 23,771.48 ha to 22,354.28 ha between

2015 and 2020. Similarly, the changes in green space area were not notably significant. From 2005 to 2011, there was an increase in green space area from 9,813.25 ha to 12,639.38 ha. However, between 2011 and 2015, there was a decrease in green space area from 12,639.38 ha to 5,178.09 ha, followed by an increase from 5,178.09 ha to 7,830.70 ha thereafter. Finally, changes in water area from 2015 to 2020 were also deemed insignificant. Specifically, from 2005 to 2011, the water area decreased from 4,907.67 ha to 4,070.93 ha. Subsequently, between 2011 and 2015, there was an increase in water area from 4,070.93 ha to 4,173.92 ha, followed by a decrease from 4,173.92 ha to 3,461.02 ha between 2015 and 2020.

Table 4 depicts the changes in area between the periods of 2005-2011, 2011-2015, and 2015-2020. Specifically, in the urban areas, there was a decrease in area of 1,987.72 ha from 2005-2011, followed by an increase of 7,423.09 ha from 2011-2015, and a subsequent decrease of 1,417.20 ha from 2015-2020. For green space areas, there was an increase in land area of 2,826.13 ha from 2005-2011, a decrease of 7,461.29 ha from 2011-2015, and a subsequent increase of 2,652.61 ha from 2015-2020. Lastly, in water areas, there was a decrease in area of 836.74 ha from 2005-2011, an increase of 102.99 ha from 2011-2015, and a subsequent decrease of 712.99 ha from 2015-2020.

Urbanization and economic development are factors of land change that occurred in Surabaya City from 2005 to 2020. This is due to population growth which causes increased demand for housing and public facilities (Kusuma et al., 2020). An example of a development case caused by population growth is the expansion of housing in the West Surabaya and East Surabaya areas, which causes land change (Setyawati et al., 2022). In addition, infrastructure development that took place in Surabaya such as the construction of the Surabaya Mojokerto Toll Road in 2007 also played a major role in land change from agricultural areas to road access (Handayani et al., 2017). The construction of the Suramadu bridge is also a cause of land change, namely the reduction of forest and vegetation by 8,130 ha from 45,924 ha to 37,794 ha (Sugiarto and Kebumian, 2018). This accelerated access to public transportation, resulting in an increase in economic activity in Surabaya City. In addition, the development of new industrial areas has caused land conversion from agricultural areas to industrial areas. The local government made changes to spatial policies that regulate industrial and commercial zones, which led to peripheral areas becoming new economic centers. The expansion of economic areas due to several combined factors is the main cause of land change (Saputra et al., 2023).

Kappa serves as a comparison between the overall accuracy value and the total accuracy expected (expected accuracy) (Wafdan, 2020). The kappa coefficient value ranges from 0.1 to 1.0, where a value closer to 1 signifies a higher level of similarity or more accurate classification of the classification results (Kushardono, 2017). In this study, the kappa coefficients for the land use classifications were calculated to be approximately 0.87%, 0.84%, 0.84%, and 0.84%, respectively (Table 5). Notably, all three classified images exhibited kappa coefficient values greater than 0.80%, indicating the accuracy of the classification estimates.

Clustering analysis is a statistical technique used to group objects or data into homogeneous groups based on the similarity of certain characteristics or attributes. Clustering analysis consists of z-score and p-value. Z-score in clustering analysis assesses how far the data values in a dataset differ from the average or random pattern. A larger z-score indicates a more significant clustering pattern. P-value in the context of clustering analysis is used to assess the statistical significance of the clustering results. With p-value equal to 0.00, the z-score values in 2005, 2011, 2015, and 2020 are 9.38, 9.43, 7.2, and 8.35, respectively (see Table 5).

Table 5. Assessment of LULC accuracy and clustering analysis.

Year	LULC Accuracy		Clustering Analysis	
	Overall Accuracy	Kappa Accuracy	z-score	p-value
2005	0.93	0.87	9.38	0.00
2011	0.91	0.84	9.43	0.00
2015	0.92	0.84	7.20	0.00
2020	0.92	0.84	8.35	0.00

3.2 Land Surface Temperature

The spatial distribution of LST in the city of Surabaya for the years 2005, 2011, 2015, and 2020 is depicted in Fig. 3b. LST values are classified into four categories: (i) below 20°C; (ii) 20–25°C; (iii) 25–30°C; and (iv) above 30°C (Ullah et al., 2022). It is important to note that there is no fixed class division for LST due to the variability in LST across different regions and time spans (Mansourmoghaddam et al., 2023). Therefore, for ease of analysis and to capture the differences in LST levels in Surabaya, the class divisions are determined based on the data obtained.

The estimated total area with temperatures below 25°C is approximately 247.70 ha in 2005, 16.20 ha in 2011, 59.53 ha in 2015, and 75.46 ha in 2020. In the temperature range of 20-25°C, the total estimated area is around 26,720.25 ha in 2005, 5,794 ha in 2011, 12,181.68 ha in 2015, and 9,864.7 ha in 2020. Similarly, for the temperature range of 25–30°C, the estimated total area is approximately 6,701.27 ha in 2005, 22,864.49 ha in 2011, 21,408.94 ha in 2015, and 23,688.13 ha in 2020. Additionally, areas with temperatures above 30°C are estimated to cover approximately 1.11 ha in 2005, 4,993.43 ha in 2011, 18.92 ha in 2015, and 38.95 ha in 2020.

3.3 Normalize Difference of Vegetation (NDVI) and Build-Up Index (NDBI)

NDVI values were categorized into four classes: (i) < 0.25; (ii) $0.26 - 0.45$; (iii) $0.46 - 0.59$; and (iv) > 0.6 to evaluate the vegetation index in the study area (see Fig. 4a).

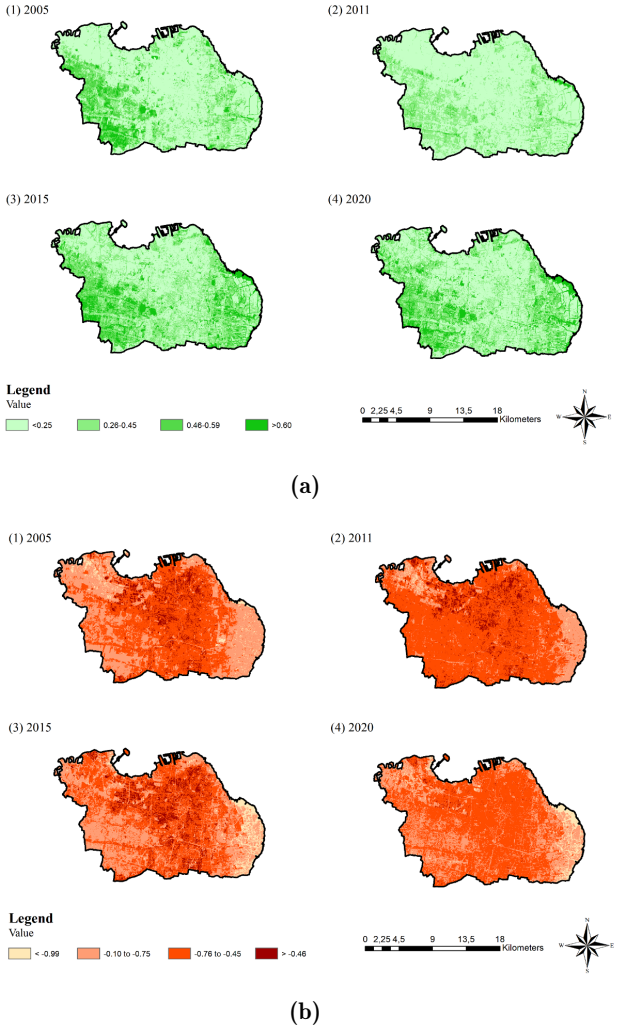

Figure 4. Illustration of (a) NDVI map in Surabaya during 2005, 2011, 2015, and 2020 and (b) NDBI map in Surabaya during 2005, 2011, 2015, and 2020.

The total area included in the < 0.25 class was estimated to be around 20837.46 ha, 24134.53 ha, 14082.62 ha, and 15967.37 ha during 2005-2020 (see Table 4). In the $(0.26 - 0.45)$ class, the area was estimated to be around 7,183.75 ha, 8,279.59 ha, 11,375.89 ha, and 10,038.27 ha. For the $(0.46 - 0.59)$ class, it was estimated to have an area of around 4,054.47 ha, 1,104.62 ha, 4,870.43 ha, and 4,621.21 ha. Meanwhile, the class > 0.60 was estimated to have an area of around 1,588.80 ha, 145.69 ha, 3,333.60 ha, and 3,035.70 ha across the years 2005, 2011, 2015, and 2020, respectively.

NDBI values were classified into four classes: (i) < -0.99; (ii) -0.10 to -0.75; (iii) -0.76 to -0.45; and (iv) > -0.46 (see Fig. 4b). The total area encompassed in the < -0.99 class was estimated to be around 817.21 ha, 288.36 ha, 1,728.31 ha, and 1,571.48 ha during the years 2005, 2011, 2015, and 2020 (see Table 4). The area in the second class (-0.10 to -0.75) was estimated at around 13,428.25 ha, 5,995.69 ha, 13,088.11 ha, and 11,309.23 ha. Meanwhile, the area for the third class (-0.76 to -0.45) was estimated to be approximately 17,228.00 ha, 25,180.96 ha, 15,971.53 ha, and 20,619.63 ha. Similarly, the > -0.46 class was estimated to have an area of around 2,189.39 ha, 2,199.24 ha, 2,875.81 ha, and 162.48 ha during the years 2005, 2011, 2015, and 2020.

3.4 Determination of Urban Heat Island

The UHI category was divided into five, namely (i) No UHI, (ii) Low, (iii) Medium, (iv) High, and (v) Very High (Dutta et al., 2021). The UHI levels in the city of Surabaya continued to change (see Fig. 5a). Changes in the level of Urban Heat Island in the City of Surabaya in 2005, 2011, 2015, and 2020 could be observed in Table 4. The land area in the No UHI category in the City of Surabaya from 2005 to 2020 was 5,223.95 ha, 2,373.53 ha, 3,861.16 ha, and 3,037.67 ha, respectively (see Table 4). In 2005, the land area with the No UHI category was the highest compared to other years. In the low category, the areas ranged from 8,759.88 ha, 24,440.2 ha, 4,960.21 ha, and 4,329.97 ha from 2005 to 2020. 2005 still recorded the highest Low UHI category among the years. Then, in the moderate category, the land area ranged from 6,833.39 ha in 2005, 5,469.73 ha in 2011, 7,390.01 ha in 2015, to 7,778.18 ha in 2020. Urban heat islands in the low category experienced a decrease in land area in 2011 and a significant increase in 2015 and 2020, surpassing the area in 2005. At the high category, urban heat islands covered areas of 9,507.40 ha, 10,859.55 ha, 9,300.40 ha, and 11,188.13 ha from 2005 to 2020. Meanwhile, the very high UHI category covered an area of 3,337.26 ha in 2005, 11,521.07 ha in 2011, 8,152.14 ha in 2015, and 7,329.42 ha in 2020. The UHI level in Surabaya City in 2011 showed a rapid increase from 2005, with 34.22% of Surabaya City classified as in the very high UHI category. Afterward, the city of Surabaya experienced a decrease in its urban heat island by 10% in several areas in 2015 and another decrease of 2.34% in 2020.

3.5 Evaluation of Urban Thermal Field Variance Index

The evaluation of the UTFVI was divided into five categories: (i) < 0.005, (ii) $0.005 - 0.010$, (iii) $0.010 - 0.015$, (iv) $0.015 - 0.020$, and (v) > 0.020 (Singh et al., 2017). The UTFVI value indicated the Ecological Evaluation Index (EEI) value (Omali, 2020), and it was further classified into five categories, namely: (i) good, (ii) normal, (iii) bad, (iv) worse, and (v) worst (see Fig. 5b).

If the UTFVI value of a land was high, it would have a significant impact on the ecological evaluation. Land in Surabaya City with a UTFVI value < 0.005 or having a good ecological evaluation impact experienced changes in land area, totaling 5,223.95 ha, 13.88 ha, 4,255.81 ha, and 3,028.23 ha from 2005 to 2020. Land with a UTFVI value of $0.005 - 0.010$ or having a normal ecological evaluation impact covered an area ranging from 8,759.88 ha, 3,512.06 ha, 5,530.82 ha, to 4,195.81 ha from 2005 to 2020.

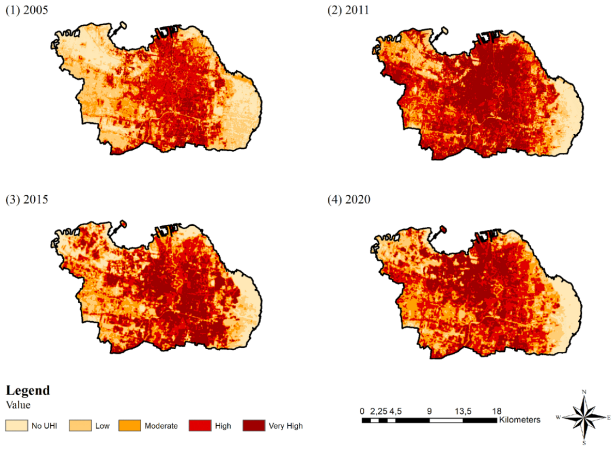

(a)

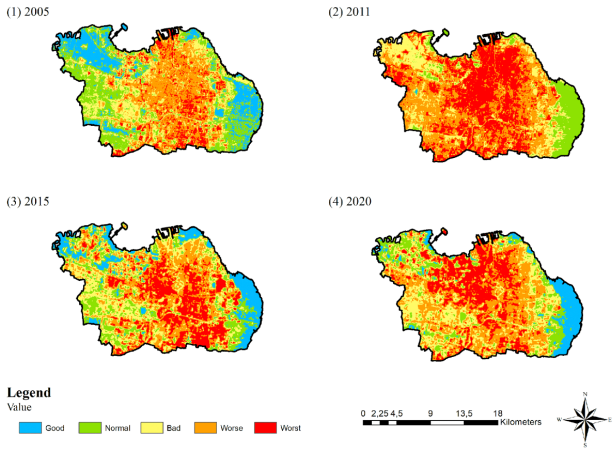

(b)

Figure 5. Illustration of (a) urban heat island (UHI) and (b) represent the Surabaya area's urban thermal variance index (UTFVI) maps during 2005, 2011, 2015, and 2020.

Meanwhile, land in the city of Surabaya from 2005 to 2020 with a UTFVI value of $0.010 - 0.015$ or having a poor ecological evaluation impact had an area of around 6,833.39 ha, 6,046.66 ha, 7,789.92 ha, and 7,900.67 ha. On land with a UTFVI value of $0.015 - 0.020$ or having a worse ecological evaluation impact, there was a significant increase and decrease in land area, totaling 9,507.40 ha in 2005, 12,576.10 ha in 2011, 9,268.19 ha in 2015, and 11,332.01 ha in 2020. Lastly, the land area of Surabaya City from 2005 to 2020, which had the worst ecological evaluation impact with a UTFVI value > 0.020, amounted to 3,337.26 ha, 11,514.45 ha, 6,819.90 ha, and 7,100.99 ha.

In 2005, UTFVI with a value of $0.010 - 0.015$ or having a worse ecological evaluation impact covered the largest land area, approximately 38.18%. In 2011, the UTFVI value for the largest land area was $0.015 - 0.020$, comprising around 37.26% of the land. Then, in 2015 and 2020, UTFVI with a value of $0.015 - 0.020$ also dominated the largest land area, accounting for 27.53% and 33.66%, respectively. It can be concluded that from 2005 to 2020, UTFVI with a value of $0.015 - 0.020$ or having a worse ecological evaluation impact dominated the land in the city of Surabaya.

3.6 Statistical Analysis

Pearson correlation analysis was utilized in this study was used to examine the relationships between the variables using IBM Statistics SPSS version 22 software (Kafle, 2019).

Table 6. Pearson correlation values between variables in 2005.

	NDBI	UTFVI	UHI	LST	NDVI
NDBI	1	0.765**	0.439**	0.053	-0.133*
		0.000	0.000	0.392	0.031
UTFVI	0.765**	1	0.612**	0.160**	-0.082
	0.000		0.000	0.010	0.183
UHI	0.439**	0.612**	1	0.114	-0.095
	0.000	0.000		0.064	0.127
LST	0.053	0.160**	0.114	1	0.080
	0.392	0.010	0.064		0.197
NDVI	-0.133*	-0.082	-0.095	0.080	1
	0.031	0.183	0.127	0.197	

Note: * Correlation is significant at the 0.05 level (2-tailed).
*** Correlation is significant at the 0.01 level (2-tailed).*

In the 2005 Pearson correlation analysis, it was observed that the correlation between NDBI and UTFVI exhibited a positive correlation, indicating a relationship between the two variables (see Table 6). Additionally, the analysis revealed positive Pearson correlations between NDBI and UHI, UTFVI and UHI, as well as UTFVI and LST (Kurniati and Nitivattananon, 2016). The positive correlation between NDBI and UTFVI suggested that higher building density corresponded to a greater impact on ecological evaluation, with higher UTFVI values indicating worse ecological impact. Similarly, the positive correlation between NDBI and UHI implied that increased building density led to higher surface temperatures in Surabaya. Moreover, the positive relationship between UTFVI and UHI, as well as UTFVI and LST, suggested that elevated surface temperatures corresponded to a heightened impact on ecological evaluation. This positive correlation indicated that urban areas like Surabaya experienced warmer cli-

mates due to extensive infrastructure development, resulting in a greater ecological impact. Conversely, a negative relationship was observed in the Pearson correlation between NDBI and NDVI, indicating an inverse proportionality where increased building density in Surabaya corresponded to lower vegetation density (Isnaeni and Prasetyo, 2022).

Pearson analysis conducted in 2011 revealed a positive correlation among various variables, including NDBI and UTFVI, NDBI and UHI, NDBI and LST, UTFVI and UHI, UTFVI and LST, as well as UHI and LST. This positive correlation indicated a directly proportional relationship between each variable (Ermawati et al., 2022). For instance, the correlation between NDBI and UTFVI suggested that higher building density corresponded to a greater ecological impact evaluation (see Table 7). The correlation value between NDBI and UTFVI in 2011 was smaller than in 2005. Moreover, the positive Pearson correlation between NDBI and UHI (Melati et al., 2020) and LST (Singh et al., 2023) indicated that increased building density in Surabaya led to higher surface temperatures in the area. Similarly, the positive relationship between the UTFVI variable and UHI and LST suggested that elevated surface temperatures in Surabaya City corresponded to a higher impact on ecological evaluation.

Table 7. Pearson correlation values between variables in 2011.

	NDBI	UTFVI	UHI	LST	NDVI
NDBI	1	0.638**	0.176**	0.053	-0.071
		0.000	0.000	0.004	0.254
UTFVI	0.638**	1	0.449**	0.251**	0.052
	0.000		0.000	0.000	0.339
UHI	0.269**	0.449**	1	0.334	0.004
	0.000	0.000		0.000	0.843
LST	0.176**	0.251**	0.334**	1	-0.008
	0.004	0.000	0.000		0.893
NDVI	-0.071	0.052	0.004	-0.008	1
	0.254	0.399	0.943	0.893	

Note: ** Correlation is significant at the 0.01 level (2-tailed).

The 2015 Pearson correlation analysis results revealed both positive and negative relationships among variables (see Table 8). Positive correlations were observed between NDBI and UTFVI, NDBI and UHI, NDBI and LST, UTFVI and UHI, UTFVI and LST, as well as UHI and LST. The positive correlation between NDBI and UTFVI, consistent with previous years, indicated a direct relationship (Hadibasyir and Firdaus, 2023); higher building density in Surabaya corresponded to increased ecological impact. Additionally, the positive Pearson correlation between NDBI and UHI variables showed higher values compared to 2011 and 2005, indicating that greater building density in Surabaya resulted in higher surface temperatures in the area. Similarly, the positive correlation between NDBI and LST, albeit with a smaller correlation value in 2015 than in 2011, suggested a direct relationship Florim et al. (2021); higher building density corresponded to higher surface temperatures. This relationship stemmed from surfaces like buildings and roads absorbing more solar radiation heat than vegetation (Estoque and Murayama, 2017). Furthermore, the positive Pearson correlation between UTFVI and LST, as well as UTFVI and UHI, indicated that higher surface temperatures in Surabaya corresponded to increased ecological impact. The positive correlation between UHI and LST suggested that higher surface temperatures in an area led to higher resulting temperatures (Prasetyo and Nurtyawan, 2023). On the other hand, negative correlations were observed between NDBI and NDVI, as well as UTFVI and NDVI. The negative relationship between NDBI and NDVI indicated an inverse relationship; higher building density corresponded to lower vegetation levels in Surabaya. Similarly, the negative correlation between UTFVI and NDVI suggested that lower vegetation density corresponded to increased ecological impact (Hadibasyir and Firdaus, 2023).

Table 8. Pearson correlation values between variables in 2015.

	NDBI	UTFVI	UHI	LST	NDVI
NDBI	1	0.682**	0.474**	0.144*	-0.341*
		0.000	0.000	0.019	0.000
UTFVI	0.682**	1	0.563**	0.143*	-0.170**
	0.000		0.000	0.020	0.006
UHI	0.474**	0.563**	1	0.140*	-0.108
	0.000	0.000		0.023	0.081
LST	0.144*	0.143*	0.140**	1	-0.037
	0.019	0.020	0.023		0.552
NDVI	-0.341**	-0.170**	-0.108	-0.037	1
	0.000	0.006	0.081	0.552	

Note: * Correlation is significant at the 0.05 level (2-tailed).
*** Correlation is significant at the 0.01 level (2-tailed).*

In the 2020 Pearson correlation analysis, positive relationships were observed among the variables NDBI and UTFVI, NDBI and UHI, NDBI and LST, UTFVI and UHI, UTFVI and LST, and UHI and LST (Mokarram et al., 2023; Pratiwi and Jaelani, 2021) (see Table 9). The positive correlation between NDBI and UTFVI indicated that higher building density corresponded to a greater ecological impact. Additionally, the positive relationship between NDBI and UHI, as well as NDBI and LST, suggested that higher building density was associated with elevated surface temperatures. The Pearson correlation values for NDBI with UHI and LST were the highest compared to previous years, signifying an increasing influence on surface temperature due to the growing amount of built-up land in Surabaya, resulting in a warmer climate (Achmad et al., 2019). Furthermore, the positive Pearson correlation between UTFVI with UHI and LST suggested that higher surface temperatures in Surabaya City were associated with an increased ecological impact. The positive relationship be-

tween UHI and LST indicated a directly proportional relationship, implying that higher surface temperatures resulted in higher overall temperatures. The Pearson correlation value for the UHI variable with LST was higher compared to 2015, suggesting an increasing relationship in 2020, potentially due to changes in the urban climate resulting from the use of environmentally unfriendly building materials.

Table 9. Pearson correlation values between variables in 2020.

	NDBI	UTFVI	UHI	LST	NDVI
NDBI	1	0.682**	0.557**	0.220*	-0.366*
		0.000	0.000	0.000	0.000
UTFVI	0.725**	1	0.698**	0.300*	-0.182**
	0.000		0.000	0.000	0.003
UHI	0.557**	0.563**	1	0.250**	-0.121*
	0.000	0.000		0.000	0.050
LST	0.220**	0.143*	0.250**	1	0.007
	0.019	0.020	0.000		0.910
NDVI	-0.341**	-0.170**	-0.121*	0.007	1
	0.000	0.006	0.050	0.910	

Note: * Correlation is significant at the 0.05 level (2-tailed).
*** Correlation is significant at the 0.01 level (2-tailed).*

Conversely, negative relationships were observed between NDBI and NDVI, UTFVI and NDVI, as well as UHI and NDVI. The negative correlation between NDBI and NDVI indicated an inverse relationship, with higher building density corresponding to lower vegetation density in Surabaya (Hadibasyir and Firdaus, 2023). Furthermore, the negative relationship between UTFVI and NDVI suggested that higher vegetation density led to a lower ecological impact. Therefore, increasing vegetation density and minimizing the area of built-up land are necessary to foster good and sustainable urban ecological conditions. Lastly, the negative relationship between UHI and NDVI indicated that lower vegetation density resulted in higher surface temperatures due to reduced vegetation, which contributed to a warmer climate. Vegetation plays a crucial role in cooling surface temperatures on land, while built-up areas tend to exacerbate the Urban Heat Island effect (Tran et al., 2017; Kumari et al., 2019).

4. Discussion

4.1 LULC, Impervious & Green Space vs Temperature

Changes in land use have been increasing due to urbanization (Saha et al., 2021). Urbanization leads to extensive development and infrastructure creation, resulting in a reduction in land cover. The shift in land use towards residential areas is driven by the growing demand for land (Adawiyah, 2021). Such changes in land cover and use due to development have a notable impact on increasing LST (Das and Angadi, 2020). This indicates a positive or harmonious relationship, wherein higher NDBI values correspond to higher LST (Sarif et al., 2020). The decrease in vegetation resulting from land use changes has repercussions on biodiversity, hydrology, and temperature. Reduced vegetation leads to an increase in temperature, contributing to the UHI phenomenon (Silva et al., 2018).

The condition of green space in Surabaya has undergone significant changes from 2005 to 2020. In 2020, green space in Surabaya accounted for only 23% of the area, falling short of the specified target. Conversely, built-up land in Surabaya constituted almost 50% of the area. Previous research has demonstrated an inverse relationship between NDVI and LST (Putra et al., 2018), indicating that decreased vegetation leads to increased land surface temperature. The rise in land surface temperatures is a key factor in the Urban Heat Island phenomenon (Pratiwi and Jaelani, 2021). Urban areas experience higher temperatures compared to rural areas (Yao et al., 2019), with Surabaya's temperatures rising due to low vegetation cover and a high concentration of buildings. The relatively high UHI value in Surabaya is evident from the majority of areas falling into the very high UHI class.

In summary, changes in LULC are primarily driven by human activities, particularly urban expansion. The transformation and expansion of cities significantly contribute to LST, with heat flow density or the intensity of uneven heat flow rates also playing a role in UHI. Converting green areas into built-up spaces poses significant risks, as the proportion of vegetation, agricultural land, and forest areas plays a crucial role in the ecosystem and urban environment (Mia et al., 2017). Green areas serve as absorbers of excess heat from urban emissions. Therefore, LULC has a profound impact on both LST and the UHI effect.

4.2 LULC, Impervious & Green Space vs UTFVI

Increasing the area of vegetation cover and green space in the urban environment has a significant influence on the thermal conditions of cities and the development of UHI (Bokaie et al., 2016). Poor temperature conditions typically resulted from the dominance of impermeable land surfaces and intense anthropogenic activities carried out in urban areas (Hadibasyir et al., 2020). Infrastructure development, such as buildings, roads, and industries, contributed to water-impermeable land cover, absorbing incoming short-wave solar radiation while reducing outgoing long-wave terrestrial emissions, thus directly impacting the Earth's surface temperature (Alademomi et al., 2022). This condition created areas known as UHI, with the strongest UHI areas directly related to more critical environments and characterized by building densification, as evidenced by the strong correlation between UTFVI and NDBI (Putra et al., 2023). UTFVI, a surface UHI measure, referred to measuring

the ecology and health of residents in urban areas (Gohain et al., 2023). It was widely used for the ecological evaluation of urban environments and was related to the Earth's surface temperature (Tepanosyan et al., 2021). The UTFVI value in urban areas accumulated higher compared to rural areas with green spaces due to the rapid pace of unplanned urban development (Kafy et al., 2021). The greater the UTFVI value, the worse the condition of urban ecological degradation and the greater the intensity of UHI, and vice versa (Hadibasyir and Firdaus, 2023). Proper planning of land cover distribution could reduce the impacts of UHI and UTFVI, promote sustainable urban development, protect ecosystem services, and improve daily life (AlDousari et al., 2022). Spatial-temporal analysis from UTFVI could be used to formulate policies and strategies for sustainable urban planning and management, mitigation and adaptation to climate change, as well as public health interventions (Kikon et al., 2023).

UTFVI, describing the urban ecological conditions of the Surabaya region, could be seen in Fig. 5a). UTFVI values were categorized into 5 classes, namely good, normal, bad, worse, and worst (Singh et al., 2017) as shown in Table 4. UTFVI values were positively correlated with UHI so that the higher the UTFVI value, the higher the UHI intensity and vice versa (Hadibasyir et al., 2020). Low UTFVI values of less than 0.005 were generally distributed in areas of water bodies and green space, indicating relatively good urban ecological quality due to the presence of mangrove vegetation (Syamsu et al., 2018). Based on the quantitative ecological assessment in the study area, namely Surabaya City (see Table 4) during 2005, 2011, 2015, and 2020, it was observed that the Surabaya area was classified in the worst category with a UTFVI value of $0.015 - 0.020$. UTFVI occurred most often in the central study area because it experienced the most urbanization and had an urban structure (Omali, 2020).

4.3 NDVI, NDBI, Impervious & Green Space vs Temperature

The temperature that describes the condition of the Surabaya area can be seen in Fig. 3b). Temperature values are categorized into 4 classes, namely $< 20°$C, 20-25°C, 25-30°C, and $> 30°$C which can be seen in Table 4. The NDVI value has an inverse relationship, which means that if the vegetation density is low, the temperature conditions will increase (Izah et al., 2023). Meanwhile, NDBI has a positive relationship with temperature where built-up areas produce many temperature variations that tend to increase and are a major contributor to urban heat island (Malik et al., 2019). Based on the quantitative ecological assessment of the study area (see Table 4) during 2005, 2011, 2015, and 2020, the Surabaya area is classified as rather high, which has a temperature between 25-30°C. As in Prayogo (2021), the Surabaya area has an average temperature above 28°C.

The natural phenomena of El Nino and La Nina have an impact on fluctuations in agriculture production. In 2011, agriculture production decreased due to the El Nino event (Mulyaqin, 2020). Conversely, La Nina resulted in an increase in rice production and a decrease in corn production (Mulyaqin, 2020). The NDVI results in 2011 had a lower density compared to other years, namely 2005, 2011, 2015, 2020 because they were influenced by the acquisition of Landsat imagery during the El Nino phenomenon. In addition, the temperature results in 2011 also showed higher than other years, namely temperatures $> 30°$C as much as 14.83% while other years were less than 1%. The El Nino phenomenon causes sea surface temperatures to increase, resulting in dry weather conditions in Indonesia. This has an impact on several areas experiencing drought, inhibiting vegetation growth and crop yields. The climate conditions that occurred in September 2011 had an impact on the acquisition of land images and the difficulty of NDVI classification.

4.4 Current Research Trends in UHI Mitigation and Adaptation

The rise in temperature attributed to global warming necessitates careful consideration. Vegetation-based green spaces play a crucial role in maintaining equilibrium on the Earth's surface temperature. Insufficient green open spaces in Indonesian, also known as Ruang Terbuka Hijau (RTH), can lead to heightened surface temperatures, resulting in discomfort (Marsitha Barung et al., 2021). This temperature increase exacerbates UHI effects, underscoring the need for mitigation and adaptation efforts. Mitigation efforts are primarily concentrated in transportation, building, industrial, energy, and governance sectors, while adaptation strategies focus on water and green infrastructure sectors in land use planning (Alizadeh and Sharifi, 2020). Utilizing green infrastructure, such as green roofs and parks, offers ecosystem benefits by mitigating UHI-induced hot climates. Green spaces, like parks, should be integrated into urban landscapes to curb rising surface temperatures. Expanding green open spaces directly reduces urban density, while tree planting provides shade during dry seasons and diminishes the sun's radiation effects, consequently mitigating UHI (Demuzere et al., 2014). Sustainable development initiatives should prioritize policies aimed at expanding green spaces with adequate vegetation, which absorb solar radiation and air pollutants. Converting vegetation areas into built-up land intensifies evapotranspiration (Achmad et al., 2019). The form of green spaces should adapt to existing land conditions; for instance, narrow land parcels can be tarnsformed into urban forest strips, while large tracts can be developed into clustered urban forests (Rushayati et al., 2016).

Green space planning extends beyond city centers to

encompass all directions of urban expansion, ensuring equitable regional growth. Additionally, green infrastructure implementation, complemented by blue infrastructure, strategically manages water usage (Almaaitah et al., 2021). Integrating water elements with sustainable maintenance practices, such as evapotranspiration, helps cool the environment, thus addressing UHI exacerbated by drought conditions (Leal Filho et al., 2018). Effective urban governance is pivotal in UHI mitigation; retro-reflective materials deflect solar radiation away from cities (O'Malley et al., 2015). Proper urban planning dictates that buildings in urban areas facilitate unimpeded wind passage and airflow, enhancing natural cooling mechanisms (Kurniati and Nitivattananon, 2016). Balancing environmental concerns with urban development presents a challenge to city planners and governments striving to minimize UHI impacts. Urban planning should not only prioritize economic factors but also optimize city layouts to mitigate UHI effects (Kurniati and Nitivattananon, 2016).

Additional mitigation measures involve reducing air conditioning and electrical energy consumption, which can exacerbate greenhouse gas effects.Strategies needed to reduce the increase in urban climate due to increased urban activity include providing green open space which can help reduce the heat island effect by providing areas that absorb and evaporate moisture (Park et al., 2022). Apart from that, cross ventilation is provided which aims to reduce heat absorption by the building (Cuce et al., 2019). There are also educational and promotional strategies for the public to preserve the environment, such as using public transportation to reduce air pollution, implementing green infrastructure, etc. (Kumari et al., 2019).

5. Conclusion

This study demonstrated a satellite-based method for observing Urban Heat Island (UHI) phenomena. The study showcases how satellite imagery can be utilized to estimate UHI occurrences during the years 2005, 2011, 2015, and 2020. It was observed that land use changes from green spaces to urban areas were a primary driver of increased Land Surface Temperature (LST). The rise in LST was found to be positively correlated with Normalized Difference Built-up Index, Urban Thermal Field Variance Index, and UHI. Conversely, an increase in LST exhibited a negative correlation with Normalized Difference Vegetation Index. This negative correlation stems from the inverse relationship between building density and vegetation density, leading to elevated urban temperatures and subsequent ecological impacts. Therefore, implementing mitigation and adaptation strategies, such as green and blue infrastructure, is imperative to counteract rising temperatures and restore equilibrium to the Earth's surface temperature. For future studies, it is recommended to use imagery with higher resolution analysis to enable improvements in classification and prediction of Land Use Land Cover and UHI both at regional and global scales. In addition, future research is also recommended to integrate open source engines to be accessible such as viewing the condition of the community environment in real time.

Acknowledgments

The author would like to express his deepest gratitude to the USGS, Google Earth, and Geospatial who have permitted the collection of Landsat imagery data as well as all parties who have been involved in preparing this research article.

CRediT authorship contribution statement

Risma Salsabila Foresty: Formal analysis, Visualization, Resources, Investigation, Writing - Original Draft. **Rida Ayu Surya Putri**: Visualization, Resources, Investigation, Writing – Original Draft. **Ririn Nur Fadhilah**:, Visualization, Writing – Original Draft, Resources, Investigation. **Salma Kamiliya Fatin:** Visualization, Investigation, Writing - Original Draft, Resources. **Muhammad Nur Sulton**: Conceptualization, Validation, Writing – Review & Editing, Data Curation. **Ahmad Dwi Setyawan**: Conceptualization, Supervisor.

Declaration of Competing Interest

The authors declare that they have no known competing financial interests or personal relationships that could have appeared to influence the work reported in this paper.

Abbreviations

The following abbreviations are used in this manuscript:

Abbreviation	Description
EEI	Ecological Evaluation Index
LST	Land Surface Temperature
LULC	Land Use Land Cover
NDBI	Normalized Difference Built-Up Index
NDVI	Normalized Difference Vegetation Index
RTH	Recreational and Therapeutic Horticulture
SCP	Semi-automatic Classification Plugin

Abbreviation	Description
UHI	Urban Heat Island
USGS	US Geological Survey
UTFVI	Urban Thermal Field Variance Index

References

Achmad, A., Sari, L. H., and Ramli, I. (2019). A study of urban heat island of Banda Aceh City, Indonesia based on land use/cover changes and land surface temperature. *Aceh International Journal of Science and Technology*, 8(1):41–51. DOI: 10.13170/aijst.8.1.13060.

Adawiyah, H. (2021). Analisis sistem informasi geografis perubahan penggunaan lahan di kecamatan labuhan haji. *Geodika: Jurnal Kajian Ilmu dan Pendidikan Geografi*, 5(1):174–184. DOI: 10.29408/geodika.v5i1.3674.

Alademomi, A. S., Okolie, C. J., Daramola, O. E., Akinnusi, S. A., Adediran, E., Olanrewaju, H. O., Alabi, A. O., Salami, T. J., and Odumosu, J. (2022). The interrelationship between LST, NDVI, NDBI, and land cover change in a section of lagos metropolis, nigeria. *Applied Geomatics*, 14(2):299–314. DOI: 10.1007/s12518-022-00434-2.

AlDousari, A. E., Kafy, A. A., Saha, M., Fattah, M. A., Almulhim, A. I., Faisal, A.-A., Al Rakib, A., Jahir, D. M. A., Rahaman, Z. A., Bakshi, A., Shahrier, M., and Rahman, M. M. (2022). Modelling the impacts of land use/land cover changing pattern on urban thermal characteristics in Kuwait. *Sustainable Cities and Society*, 86:104107. DOI: 10.1016/j.scs.2022.104107.

Alizadeh, H. and Sharifi, A. (2020). Assessing resilience of urban critical infrastructure networks: A case study of Ahvaz, Iran. *Sustainability*, 12(9):3691. DOI: 10.3390/su12093691.

Almaaitah, T., Appleby, M., Rosenblat, H., Drake, J., and Joksimovic, D. (2021). The potential of blue-green infrastructure as a climate change adaptation strategy: A systematic literature review. *Blue-Green Systems*, 3(1):223–248. DOI: 10.2166/bgs.2021.016.

Bala, R., Prasad, R., and Yadav, V. P. (2021). Quantification of urban heat intensity with land use/land cover changes using landsat satellite data over urban landscapes. *Theoretical and Applied Climatology*, 145(1–2):1–12. DOI: 10.1007/s00704-021-03610-3.

Bokaie, M., Zarkesh, M. K., Arasteh, P. D., and Hosseini, A. (2016). Assessment of urban heat island based on the relationship between land surface temperature and land use/ land cover in Tehran. *Sustainable Cities and Society*, 23:94–104. DOI: 10.1016/j.scs.2016.03.009.

Chairuman, M., Wihadanto, A., and Rusdiyanto, E. (2023). Perubahan penggunaan lahan Perkotaan dan fenomena urban heat island di Kota Tangerang Selatan. *ULIN: Jurnal Hutan Tropis*, 7(2):142. DOI: 10.32522/ujht.v7i2.10375.

Choudhury, D., Das, K., and Das, A. (2019). Assessment of land use land cover changes and its impact on variations of land surface temperature in Asansol-Durgapur development region. *The Egyptian Journal of Remote Sensing and Space Science*, 22(2):203–218. DOI: 10.1016/j.ejrs.2018.05.004.

Chung, J., Lee, Y., Jang, W., Lee, S., and Kim, S. (2020). Correlation analysis between air temperature and MODIS land surface temperature and prediction of air temperature using TensorFlow long short-term memory for the period of occurrence of cold and heat waves. *Remote Sensing*, 12(19):3231. DOI: 10.3390/rs12193231.

Congedo, L. (2021). Semi-automatic classification plugin: A python tool for the download and processing of remote sensing images in QGIS. *Journal of Open Source Software*, 6(64):3172. DOI: 10.21105/joss.03172.

Cuce, E., Sher, F., Sadiq, H., Cuce, P. M., Guclu, T., and Besir, A. B. (2019). Sustainable ventilation strategies in buildings: CFD research. *Sustainable Energy Technologies and Assessments*, 36:100540. DOI: 10.1016/j.seta.2019.100540.

Das, S. and Angadi, D. P. (2020). Land use-land cover (LULC) transformation and its relation with land surface temperature changes: A case study of barrackpore subdivision, West Bengal, India. *Remote Sensing Applications: Society and Environment*, 19:100322. DOI: 10.1016/j.rsase.2020.100322.

Dash, P., Sanders, S. L., Parajuli, P., and Ouyang, Y. (2023). Improving the accuracy of land use and land cover classification of landsat data in an agricultural watershed. *Remote Sensing*, 15(16):4020. DOI: 10.3390/rs15164020.

Demuzere, M., Orru, K., Heidrich, O., Olazabal, E., Geneletti, D., Orru, H., Bhave, A., Mittal, N., Feliu, E., and Faehnle, M. (2014). Mitigating and adapting to climate change: Multi-functional and multi-scale assessment of green urban infrastructure. *Journal of Environmental Management*, 146:107–115. DOI: 10.1016/j.jenvman.2014.07.025.

Dutta, K., Basu, D., and Agrawal, S. (2021). Evaluation of seasonal variability in magnitude of urban heat islands using local climate zone classification and surface albedo. *International Journal of Environmental Science and Technology*, 19(9):8677–8698. DOI: 10.1007/s13762-021-03602-w.

Ermawati, M., Syahputra, A., and Mutmainah, T. (2022). Analisis faktor-faktor yang mempengaruhi urban heat island di kota bandarlampung. *Reka Ruang*, 5(2):54–66.

Estoque, R. C. and Murayama, Y. (2017). Monitoring surface urban heat island formation in a tropical mountain city using Landsat data (1987–2015). *ISPRS Journal of Photogrammetry and Remote Sensing*, 133:18–29. DOI: 10.1016/j.isprsjprs.2017.09.008.

Faza Illiyin, D., Martokusumo, W., and Donny Koerniawan, M. (2019). Analysis of correlation betweeen urban structure parameters and climatic variables in heritage area of Rajawali-Surabaya as urban heat island mitigation. *KnE Social Sciences*. DOI: 10.18502/kss.v3i21.4969.

Florim, I., Albert, B., and Shpejtim, B. (2021). Measuring UHI using Landsat-8 OLI and TIRS data with NDVI and NDBI in municipality of Prishtina. *Disaster Advances*, 14(11):25–36.

Gandhi, G. M., Parthiban, S., Thummalu, N., and Christy, A. (2015). Ndvi: Vegetation change detection using remote sensing and Gis – A case study of Vellore District. *Procedia Computer Science*, 57:1199–1210. DOI: 10.1016/j.procs.2015.07.415.

Gohain, K. J., Goswami, A., Mohammad, P., and Kumar, S. (2023). Modelling relationship between land use land cover changes, land surface temperature and urban heat island in Indore city of central India. *Theoretical and Applied Climatology*, 151(3–4):1981–2000. DOI: 10.1007/s00704-023-04371-x.

Gunathilaka, M. D. K. L. and Harshana, W. T. S. (2021). Evaluation of urban heat island (UHI) spatial change in freshwater lakes with hot spot analysis (GI statistics). *International Journal of Environment, Engineering and Education*, 3(2):48–58. DOI: 10.55151/ijeedu.v3i2.54.

Hadibasyir, H. Z., Fikriyah, V. N., Sunariya, M. I. T., and Danardono, D. (2020). Pemetaan kondisi ekologi perkotaan skala mikro menggunakan citra Landsat 8 di kota semarang. *LaGeografia*, 18(3):209. DOI: 10.35580/lageografia.v18i3.13476.

Hadibasyir, H. Z. and Firdaus, N. S. (2023). Spatial analysis of urban ecological condition in Denpasar city, Indonesia using Landsat 9 imagery. *Jurnal Purifikasi*, 21(1):38–44. DOI: 10.12962/j25983806.v21.i1.429.

Handayani, M. F., Parsudi, S., and Sudarto, T. (2017). Dampak pembebasan lahan pertanian untuk jalan tol Surabaya - mojokerto (sumo) terhadap kualitas hidup petani bekas pemilik lahan di sumberwaru, wringinanom – gresik. *Berkala Ilmiah Agridevina*, 5(2). DOI: 10.33005/adv.v5i2.820.

Islami, F. A., Tarigan, S. D., Wahjunie, E. D., and Dasanto, B. D. (2022). Accuracy assessment of land use change analysis using Google Earth in Sadar Watershed Mojokerto regency. *IOP Conference Series: Earth and Environmental Science*, 950(1):012091. DOI: 10.1088/1755-1315/950/1/012091.

Isnaeni, A. Y. and Prasetyo, S. Y. J. (2022). Klasifikasi wilayah potensi risiko kerusakan lahan akibat bencana tsunami menggunakan machine learning. *Jurnal Teknik Informatika dan Sistem Informasi*, 8(1). DOI: 10.28932/jutisi.v8i1.4056.

Izah, A., Shafarani, F. K., Afrianto, F., and Permana, M. (2023). Hubungan antara kepadatan vegetasi dan land surface temperature di kabupaten pasuruan. *Jurnal Plano Buana*, 4(1):12–21.

Ji, Y., Zhan, W., Du, H., Wang, S., Li, L., Xiao, J., Liu, Z., Huang, F., and Jin, J. (2023). Urban-rural gradient in vegetation phenology changes of over 1500 cities across China jointly regulated by urbanization and climate change. *ISPRS Journal of Photogrammetry and Remote Sensing*, 205:367–384. DOI: 10.1016/j.isprsjprs.2023.10.015.

Kafle, S. C. (2019). Correlation and regression analysis using spss. *Management, Technology & Social Sciences*, page 126. Retrieved from Oxford College Journal.

Kafy, A. A., Abdullah-Al-Faisal, Rahman, M. S., Islam, M., Al Rakib, A., Islam, M. A., Khan, M. H. H., Sikdar, M. S., Sarker, M. H. S., Mawa, J., and Sattar, G. S. (2021). Prediction of seasonal urban thermal field variance index using machine learning algorithms in Cumilla, Bangladesh. *Sustainable Cities and Society*, 64:102542. DOI: 10.1016/j.scs.2020.102542.

Karakuş, C. B. (2019). The impact of land use/land cover (LULC) changes on land surface temperature in Sivas City Center and its surroundings and assessment of urban heat island. *Asia-Pacific Journal of Atmospheric Sciences*, 55(4):669–684. DOI: 10.1007/s13143-019-00109-w.

Katherina, L. K. and Indraprahasta, G. S. (2019). Urbanization pattern in Indonesia's secondary cities: Greater Surabaya and its path toward a megacity. *IOP Conference Series: Earth and Environmental Science*, 338(1):012018. DOI: 10.1088/1755-1315/338/1/012018.

Khafid, M. A., Wicaksono, A. P., and Dewantoro, B. E. B. (2020). Method of land cover change and number of vehicles increasing on land surface temperature: Case research of Surabaya City, East Java Province, Indonesia. *International Journal of Innovative Technology and Exploring Engineering*, 9(3S):177–181. DOI: 10.35940/ijitee.c1039.0193s20.

Khamchiangta, D. and Dhakal, S. (2020). Time series analysis of land use and land cover changes related to urban heat island intensity: Case of Bangkok metropolitan area in Thailand. *Journal of Urban Management*, 9(4):383–395. DOI: 10.1016/j.jum.2020.09.001.

Khanh, D. N., Varquez, A. C., and Kanda, M. (2023). Impact of urbanization on exposure to extreme warming in megacities. *Heliyon*, 9(4):e15511. DOI: 10.1016/j.heliyon.2023.e15511.

Kikon, N., Kumar, D., and Ahmed, S. A. (2023). Quantitative assessment of land surface temperature and vegetation indices on a kilometer grid scale. *Environmental Science and Pollution Research*, 30(49):107236–107258. DOI: 10.1007/s11356-023-27418-y.

Kumari, M., Sarma, K., and Sharma, R. (2019). Using Moran's I and GIS to study the spatial pattern of land surface temperature in relation to land use/-cover around a thermal power plant in Singrauli district, Madhya Pradesh, India. *Remote Sensing Applications: Society and Environment*, 15:100239. DOI: 10.1016/j.rsase.2019.100239.

Kurniati, A. C. and Nitivattananon, V. (2016). Factors influencing urban heat island in Surabaya, Indonesia. *Sustainable Cities and Society*, 27:99–105. DOI: 10.1016/j.scs.2016.07.006.

Kushardono, D. (2017). *Klasifikasi Digital pada Penginderaan Jauh*. IPB Press, Bogor, Indonesia.

Kusuma, R. D., Purnomo, E. P., and Kasiwi, A. N. (2020). Analisis upaya kota Surabaya untuk mewujudkan kota hijau (green city). *Dinamika : Jurnal Ilmiah Ilmu Administrasi Negara*, 7(1):13–27. DOI: 10.25157/dinamika.v7i1.3173.

Leal Filho, W., Echevarria Icaza, L., Neht, A., Klavins, M., and Morgan, E. A. (2018). Coping with the impacts of urban heat islands. A literature based study on understanding urban heat vulnerability and the need for resilience in cities in a global climate change context. *Journal of Cleaner Production*, 171:1140–1149. DOI: 10.1016/j.jclepro.2017.10.086.

Malik, M. S., Shukla, J. P., and Mishra, S. (2019). Relationship of LST, NDBI and NDVI using Landsat-8 data in Kandaihimmat watershed, Hoshangabad, India. *Indian Journal of Geo Marine Science*, 48(1):25–31.

Marsitha Barung, F., Jan Pattipeilohy, W., and Muharsyah, R. (2021). Assessment of climate change based on annual trend and change of temperature in manokwari, west papua. *Jurnal Analisis Kebijakan Kehutanan*, 18(1):45–57. DOI: 10.20886/jakk.2021.18.1.45-57.

Melati, F. S., Sukmono, A., and Bashit, N. (2020). Analisis pengaruh perubahan densifikasi bangunan terhadap fenomena urban heat island menggunakan algoritma urban index dengan citra landsat multitemporal (studi kasus: Kota pekalongan). *Jurnal Geodesi Undip*, 9:166–175.

Mia, B., Bhattacharya, R., and Woobaidullah, A. (2017). Urban heat island with land use-land cover of Dhaka City using satellite imageries. *International Journal of Research in Geography*, 3(4). DOI: 10.20431/2454-8685.0304002.

Moazzam, M. F. U., Doh, Y. H., and Lee, B. G. (2022). Impact of urbanization on land surface temperature and surface urban heat island using optical remote sensing data: A case study of jeju island, republic of korea. *Building and Environment*, 222:109368. DOI: 10.1016/j.buildenv.2022.109368.

Mokarram, M., Taripanah, F., and Pham, T. M. (2023). Investigating the effect of surface urban heat island on the trend of temperature changes. *Advances in Space Research*, 72(8):3150–3169. DOI: 10.1016/j.asr.2023.06.048.

Mulyaqin, T. (2020). Pengaruh el nino dan la nina terhadap fluktuasi produksi padi di provinsi banten. *Jurnal Agromet*, 34(1):34–41.

Nailufar, B. (2018). Analisis perubahan indeks kerapatan vegetasi dengan metode analisis normalized difference vegetation index (NDVI) di kota batu berbasis sistem informasi geografis (GIS) dan pengindraan jauh. *Mintakat: Jurnal Arsitektur*, 19(2). DOI: 10.26905/mintakat.v19i2.2356.

Noviyanti, E. and Santoso, E. B. (2016). Factors affect of urban heat island from city form and city function in downtown Surabaya City (UP. Tunjungan). *International Journal of Engineering Research & Technology*, 5(1):345–352. DOI: 10.17577/IJERTV5IS010262.

Olofsson, P., Foody, G. M., Herold, M., Stehman, S. V., Woodcock, C. E., and Wulder, M. A. (2014). Good practices for estimating area and assessing accuracy of land change. *Remote Sensing of Environment*, 148:42–57. DOI: 10.1016/j.rse.2014.02.015.

Omali, T. U. (2020). Ecological evaluation of urban heat island impacts in Abuja municipal area of FCT Abuja, Nigeria. *World Academics Journal of Engineering Sciences*, 7:66–72.

O'Malley, C., Piroozfar, P., Farr, E. R., and Pomponi, F. (2015). Urban heat island (UHI) mitigating strategies: A case-based comparative analysis. *Sustainable Cities and Society*, 19:222–235. DOI: 10.1016/j.scs.2015.05.009.

Pan, Y., Zhang, H., Wang, C., and Zhou, Y. (2023). Impact of land use change on regional carbon sink capacity: Evidence from Sanmenxia, China. *Ecological Indicators*, 156:111189. DOI: 10.1016/j.ecolind.2023.111189.

Park, J., Shin, Y., Kim, S., Lee, S.-W., and An, K. (2022). Efficient plant types and coverage rates for optimal green roof to reduce urban heat island effect. *Sustainability*, 14(4):2146. DOI: 10.3390/su14042146.

Prasetyo, B. D. and Nurtyawan, R. (2023). Analisis urban heat island di kota semarang berdasarkan hubungan kerapatan vegetasi dan keterbangunan kota terhadap suhu permukaan. In *Prosiding FTSP Series*, pages 284–289.

Pratiwi, A. Y. and Jaelani, L. M. (2021). Analisis perubahan distribusi urban heat island (UHI) di kota Surabaya menggunakan citra satelit Landsat multitemporal. *Jurnal Teknik ITS*, 9(2):48–55.

Prayogo, L. M. (2021). Platform Google Earth engine untuk pemetaan suhu permukaan daratan dari data series modis. *DoubleClick: Journal of Computer and Information Technology*, 5(1):25. DOI: 10.25273/doubleclick.v5i1.8604.

Putra, A. K., Sukmono, A., and Sasmito, B. (2018). Analisis hubungan perubahan tutupan lahan terhadap suhu permukaan terkait fenomena urban heat island menggunakan citra landsat (studi kasus: Kota surakarta). *Jurnal Geodesi Undip*, 7(3):22–31. DOI: 10.14710/jgundip.2018.21212.

Putra, I. K. G. A. P., Risdiyanto, I., and Hidayat, R. (2023). Correlation analysis between urban heat island intensity and temperature criticality value in Denpasar City. *Agromet*, 37(2):66–76. DOI: 10.29244/j.agromet.37.2.66-76.

Rahardian, D. and Ruslana, d. Z. N. (2022). Hubungan antara kerapatan dan jenis vegetasi terhadap kejadian angin puting beliung di kabupaten kendal tahun 2017-2021. *Buletin Meteorologi, Klimatologi dan Geofisika*, 2(6):25–34.

Rushayati, S. B., Prasetyo, L. B., Puspaningsih, N., and Rachmawati, E. (2016). Adaptation strategy toward urban heat island at tropical urban area. *Procedia Environmental Sciences*, 33:221–229. DOI: 10.1016/j.proenv.2016.03.073.

Safitri, R., Vonnisa, M., and Marzuki, M. (2022). Analisis dampak perubahan tutupan lahan di kalimantan terhadap temperatur permukaan. *Jurnal Fisika Unand*, 11(2):173–179. DOI: 10.25077/jfu.11.2.173-179.2022.

Safitri, W. R. (2016). Pearson correlation analysis to determine the relationship between city population density with incident dengue fever of Surabaya in the year 2012-2014. *Jurnal Ilmiah Keperawatan (Scientific Journal of Nursing)*, 2(2):21–29.

Saha, S., Saha, A., Das, M., Saha, A., Sarkar, R., and Das, A. (2021). Analyzing spatial relationship between land use/land cover (LULC) and land surface temperature (LST) of three urban agglomerations (UAs) of Eastern India. *Remote Sensing Applications: Society and Environment*, 22:100507. DOI: 10.1016/j.rsase.2021.100507.

Saputra, A. A., Hakim, F. L., Mandala, M., and Indarto, I. (2023). Pemanfaatan citra landsat untuk pemantauan perubahan tutupan lahan lima dekade pada kawasan perkotaan dan aglomerasi industri provinsi Jawa timur. *Seminar Nasional Teknik Sipil*, 1(1):343–254.

Sari, D. P. (2021). A review of how building mitigates the urban heat island in Indonesia and tropical cities. *Earth*, 2(3):653–666. DOI: 10.3390/earth2030038.

Sarif, M. O., Rimal, B., and Stork, N. E. (2020). Assessment of changes in land use/land cover and land surface temperatures and their impact on surface urban heat island phenomena in the Kathmandu Valley (1988–2018). *ISPRS International Journal of Geo-Information*, 9(12):726. DOI: 10.3390/ijgi9120726.

Sasmito, B. and Suprayogi, A. (2017). Model kekritisan indeks lingkungan dengan algoritma urban heat island Di Kota Semarang. *Majalah Ilmiah Globe*, 19(1):45. DOI: 10.24895/mig.2017.19-1.509.

Setyawati, K. C., Ghifari, M. K., and Aribahwanto, M. A. (2022). Pengaruh pengaruh urban sprawl terhadap tata kota Surabaya. *Journal of Economics Development Issues*, 5(2):78–85. DOI: 10.33005/jedi.v5i2.122.

Seun, A. I., Ayodele, A. P., Koji, D., and Akande, S. O. (2022). The potential impact of increased urbanization on land surface temperature over south-west Nigeria. *Current Research in Environmental Sustainability*, 4:100142. DOI: 10.1016/j.crsust.2022.100142.

Silva, J. S., Silva, R. M. d., and Santos, C. A. G. (2018). Spatiotemporal impact of land use/land cover changes on urban heat islands: A case study of Paço do Lumiar, Brazil. *Building and Environment*, 136:279–292. DOI: 10.1016/j.buildenv.2018.03.041.

Singh, P., Kikon, N., and Verma, P. (2017). Impact of land use change and urbanization on urban heat island in Lucknow city, Central India. A remote sensing based estimate. *Sustainable Cities and Society*, 32:100–114. DOI: 10.1016/j.scs.2017.02.018.

Singh, P., Verma, P., Chaudhuri, A. S., Singh, V. K., and Rai, P. K. (2023). Evaluating the relationship between urban heat island and temporal change in land use, NDVI and NDBI: A case study of Bhopal

city, India. *International Journal of Environmental Science and Technology*, 21(3):3061–3072. DOI: 10.1007/s13762-023-05141-y.

Sugiarto, B. O. N. I. E. and Kebumian, L. D. (2018). Prediksi perubahan tutupan lahan akibat dampak pembangunan jembatan suramadu di kabupaten bangkalan. *Jurnal Teknik Geomatika Fakultas Teknik Sipil Institut Teknologi Sepuluh Nopember*.

Syafitri, R. A. W. D., Pamungkas, A., and Santoso, E. B. (2021). Urban form factors that play important roles on UHI spatial-temporal pattern: A case study of east Surabaya, Indonesia. *IOP Conference Series: Earth and Environmental Science*, 764(1):012030. DOI: 10.1088/1755-1315/764/1/012030.

Syamsu, I. F., Nugraha, A. Z., Nugraheni, C. T., and Wahwakhi, S. A. L. M. A. N. A. (2018). Kajian perubahan tutupan lahan di ekosistem mangrove pantai timur surabaya. *Media Konservasi*, 23(2):122–131.

Taufik, A., Syed Ahmad, S. S., and Ahmad, A. (2016). Classification of Landsat 8 satellite data using NDVI tresholds. *Journal of Telecommunication, Electronic and Computer Engineering (JTEC)*, 8(4):37–40.

Tempa, K. and Aryal, K. R. (2022). Semi-automatic classification for rapid delineation of the geohazard-prone areas using Sentinel-2 satellite imagery. *SN Applied Sciences*, 4(5). DOI: 10.1007/s42452-022-05028-6.

Tepanosyan, G., Muradyan, V., Hovsepyan, A., Pinigin, G., Medvedev, A., and Asmaryan, S. (2021). Studying spatial-temporal changes and relationship of land cover and surface urban heat island derived through remote sensing in Yerevan, Armenia. *Building and Environment*, 187:107390. DOI: 10.1016/j.buildenv.2020.107390.

Tran, D. X., Pla, F., Latorre-Carmona, P., Myint, S. W., Caetano, M., and Kieu, H. V. (2017). Characterizing the relationship between land use land cover change and land surface temperature. *ISPRS Journal of Photogrammetry and Remote Sensing*, 124:119–132. DOI: 10.1016/j.isprsjprs.2017.01.001.

Ullah, N., Siddique, M. A., Ding, M., Grigoryan, S., Zhang, T., and Hu, Y. (2022). Spatiotemporal impact of urbanization on urban heat island and urban thermal field variance index of Tianjin City, China. *Buildings*, 12(4):399. DOI: 10.3390/buildings12040399.

Wafdan, L. (2020). Identifikasi klasifikasi lahan di kecamatan pakem kabupaten sleman berdasarkan intepretasi citra Sentinel-2. *Jurnal Ilmiah Penalaran dan Penelitian Mahasiswa*, 4(1):105–128.

Wu, K., Wang, D., Lu, H., and Liu, G. (2023). Temporal and spatial heterogeneity of land use, urbanization, and ecosystem service value in China: A national-scale analysis. *Journal of Cleaner Production*, 418:137911. DOI: 10.1016/j.jclepro.2023.137911.

Yao, R., Wang, L., Huang, X., Gong, W., and Xia, X. (2019). Greening in rural areas increases the surface urban heat island intensity. *Geophysical Research Letters*, 46(4):2204–2212. DOI: 10.1029/2018gl081816.

Yin, Z., Liu, Z., Liu, X., Zheng, W., and Yin, L. (2023). Urban heat islands and their effects on thermal comfort in the US: New York and New Jersey. *Ecological Indicators*, 154:110765. DOI: 10.1016/j.ecolind.2023.110765.

Ziar, H., Sönmez, F. F., Isabella, O., and Zeman, M. (2019). A comprehensive albedo model for solar energy applications: Geometric spectral albedo. *Applied Energy*, 255:113867. DOI: 10.1016/j.apenergy.2019.113867.